Two-Scale Structure of the Electron Dissipation Region
during Collisionless Magnetic Reconnection

M. A. Shay[*]

Department of Physics & Astronomy, 217 Sharp Lab, University of Delaware, Newark, Delaware 19716, USA

J. F. Drake and M. Swisdak

University of Maryland, College Park, Maryland, 20742, USA

Particle-in-cell simulations of collisionless magnetic reconnection are presented that demonstrate that reconnection remains fast in very large systems. The electron dissipation region develops a distinct two-scale structure along the outflow direction. Consistent with fast reconnection, the length of the electron current layer stabilizes and decreases with decreasing electron mass, approaching the ion inertial length for a proton-electron plasma. Surprisingly, the electrons form a super-Alfvénic outflow jet that remains decoupled from the magnetic field and extends large distances downstream from the x line.

Magnetic reconnection drives the release of magnetic energy in explosive events such as disruptions in laboratory experiments, magnetic substorms in the Earth's magnetosphere and flares in the solar corona. The rate of reconnection is controlled by a narrow boundary layer, the "dissipation region", where strong currents are driven and dissipative effects enable magnetic field lines to reconnect. Since the 1950s it has been recognized that the long and narrow dissipation region that develops in the magnetohydrodynamic (MHD) model throttles reconnection and is inconsistent with the fast energy release in observations [1,2]. In the Hall reconnection model the dissipation region shortens dramatically and produces fast reconnection as in the observations [3–5].

Recent kinetic simulations have called into question the fundamental tenets of the Hall reconnection model and therefore the current explanation of fast reconnection seen in nature [6,7]. In these simulations the electron out-of-plane current layer stretches along the outflow direction, leading to an electron flow bottleneck which causes the rate of reconnection to drop. The fast rates of reconnection obtained from earlier simulations [3,4,8] were attributed to the influence of periodicity. The conclusion of this work was that the Hall model suffers from the same fundamental flaw as the earlier MHD models of reconnection—the elongated dissipation region (electron out-of-plane current) kills fast reconnection.

In contrast, we present particle-in-cell simulations with various electron masses and computational domain sizes that demonstrate that collisionless reconnection remains fast even in very large systems. The reconnection rate stabilizes before the periodicity of the boundary conditions can impact the dynamics. The electron dissipation region develops a distinct two-scale structure along the outflow direction that had not been identified in earlier simulations. As expected from the high rates of reconnection, the out-

of-plane electron current layer stabilizes at a length that decreases with the electron mass and extrapolates to about an ion inertial length $d_i = c/\omega_{\rm pi}$ for the physical electron-proton mass ratio. The surprise is that a jet of outflowing electrons with velocity close to the electron Alfven speed $c_{\rm Ae}$ extends up to several $10s$ of d_i from the x line, growing continuously in length until the simulation ends. Remarkably, the electrons are able to jet across the magnetic field over such enormous distances because momentum transport transverse to the jet effectively "blocks" the flow of the out-of-plane current in this region. This strong momentum transport has the same source (the off diagonal pressure tensor [8]), but is much stronger than that which balances the reconnection electric field at the x line.

Our simulations are performed with the particle-in-cell code P3D [9]. The results are presented in normalized units: the magnetic field to the asymptotic value of the reversed field, the density to the value at the center of the current sheet minus the uniform background density, velocities to the Alfvén speed v_A, lengths to the ion inertial length d_i, times to the inverse ion cyclotron frequency $\Omega_{\rm ci}^{-1}$, and temperatures to $m_i v_A^2$. We consider a system periodic in the $x - y$ plane where flow into and away from the x line are parallel to $\hat{\mathbf{y}}$ and $\hat{\mathbf{x}}$, respectively. The reconnection electric field is parallel to $\hat{\mathbf{z}}$. The initial equilibrium consists of two Harris current sheets superimposed on an ambient population with a uniform density of 0.2. This configuration is chosen because it reproduces the large values of the tearing mode stability parameter Δ' that characterize the long wavelength limit of reconnection in a single current slab [10] and does not exhibit artificial saturation due to conducting boundaries [11]. The reconnection magnetic field is given by $B_x = \tanh[(y - L_y/4)/w_0] - \tanh[(y - 3L_y/4)/w_0] - 1$, where w_0 and L_y are the half-width of the initial current sheets and the box size in the $\hat{\mathbf{y}}$ direction. The electron and ion tempera-

tures, $T_e = 1/12$ and $T_i = 5/12$, are initially uniform. The simulations presented here are two-dimensional, i.e., $\partial/\partial z = 0$. While the development of turbulence in a large-scale 3D system remains an open issue, in smaller systems initiated with noise the x line elongates along $\hat{\mathbf{z}}$ and the reconnection becomes quasi-2D at late time [12]. Here reconnection is initiated with a small initial magnetic perturbation that produces a single magnetic island on each current layer.

We have explored the dependence of the rate of reconnection on the system size in a series of simulations with three different system sizes and three different mass ratios (Fig. 1). For $m_i/m_e = 25$, the grid scale $\Delta = 0.05$ and the speed of light $c = 15$. For $m_i/m_e = 100$, $\Delta = 0.025$ and $c = 20$. For $m_i/m_e = 400$, $\Delta = 0.0125$ and $c = 40$. The rate increases with time, undergoes a modest overshoot that is more pronounced in the smaller domains, and approaches a quasisteady rate of around 0.14, independent of the domain size. Changing the aspect ratio of the simulation domain does not modify the quasisteady reconnection rate. Earlier suggestions [6] that reconnection rates would plunge until elongated current layers spawned secondary magnetic islands are not borne out in these simulations. The rates of reconnection approach constant values even in the absence of secondary islands, which for anti-

FIG. 1 (color online). Reconnection electric field (time derivative of the magnetic flux between the x line and o line) versus time: (a) 204.8×102.4, (b) 102.4×51.2, (c) 51.2×25.6. w_0 is the initial current sheet width.

parallel reconnection typically only occur transiently due to initial conditions [13]. Even these transient islands can be largely eliminated by a suitable choice of the initial current layer width w_0 (a larger value of w_0 is required for the larger domains).

A critical issue is whether the periodicity in the x direction can influence the rate of reconnection [6]. In each of the simulations we have identified the time at which the ion outflows from the x line meet at the center of the magnetic island. This occurs at $t \approx 155$ for the largest simulation shown in Fig. 1(a). The plasma at the x line cannot be affected by the downstream conditions until $t \approx 255$, when a pressure perturbation can propagate back upstream to the x line. This is well after the end of the simulation. The electrons are ejected from the x line at a velocity of around $c_{Ae} \gg c_A$ and therefore might be able to follow field lines back to the x line. During the traversal time $\delta t = L_x/c_{Ae}$, the reconnected flux is $v_{in}B_0L_x/c_{Ae}$, where v_{in} is the inflow velocity into the x line. Using the conservation of the canonical momentum in the z direction, the condition that an electron with a velocity c_{Ae} can not cross this flux to access the x line reduces to $L_x > d_i(c_A/v_{in}) \sim 7d_i$, which is easily satisfied for the simulations in Fig. 1. That the reconnection rates for all of the simulation domains in Fig. 1 are essentially identical further supports this conclusion. Also shown in Fig. 1 in the dashed lines are the rates of reconnection for $m_i/m_e = 100$ in (b) and $m_i/m_e = 400$ in (c). Consistent with simulations in smaller domains [8,14], the rate of reconnection is insensitive to the electron mass.

We now proceed to explore the structure of the electron current layer. Shown in Fig. 2 is a blowup around the x line of the out-of-plane electron velocity for $m_i/m_e = 25$ (two simulation domains) and for $m_i/m_e = 400$. All of the data are taken in the phase where the reconnection rate and the lengths of the region of intense out-of-plane current are stationary. The current layers for $m_i/m_e = 25$ have half-lengths of around $7d_i$, independent of the system size, and open up downstream forming the open outflow jet that characterizes Hall reconnection [3–5]. The current layer in the case of $m_i/m_e = 400$ in Fig. 2(c) is distinctly shorter than those in Figs. 2(a) and 2(b), suggesting that the length of the electron current layer depends on the electron mass and would be even shorter for realistic proton-electron mass ratios.

Shown in Fig. 3(a) is a blowup around the x line of the electron outflow velocity v_{ex} for the run corresponding to Fig. 2(a). In contrast with the out-of-plane current the electrons form an outflow jet that extends a very large distance downstream from the x line. This outflow jet continued to grow in length until the end of the simulation. This simulation, along with others at differing mass ratios, reveals that the peak outflow velocity is very close to the electron Alfvén speed [11,15]. One might expect that because of the collimation of the outflow jet and its length,
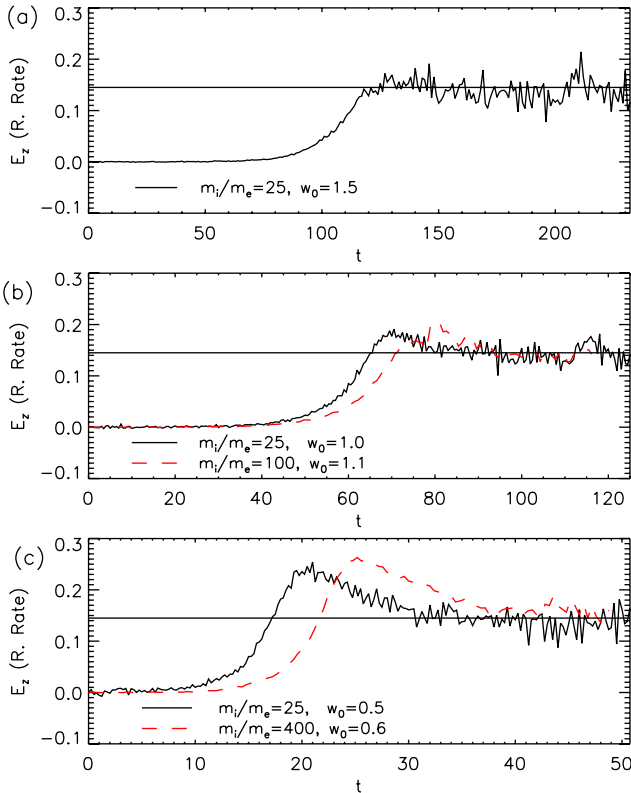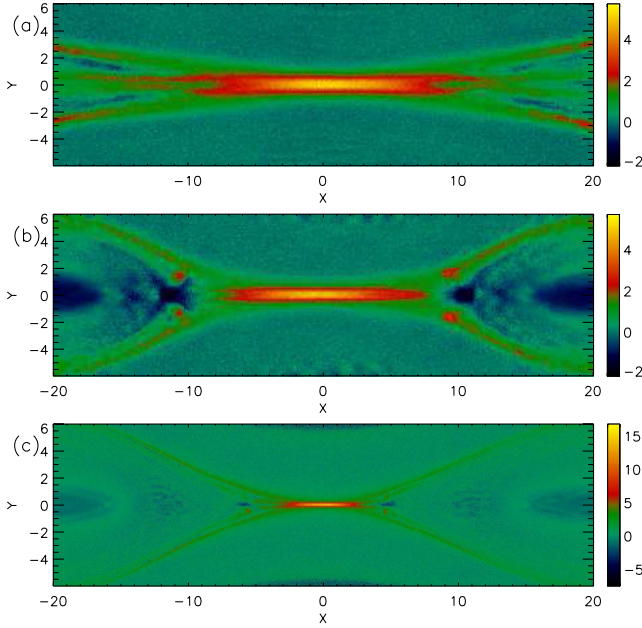
FIG. 2 (color online).   Blowups around the x line of the out-of-plane electron velocity for: (a) $m_i/m_e = 25$, simulation size 204.8×102.4, (b) $m_i/m_e = 25$, 51.2×25.6, and (c) $m_i/m_e = 400$, 51.2×25.6.

the reconnection rate would drop. However, this is not the case. While there is an intense jet in the core of the reconnection exhaust, the exhaust as a whole quickly opens up downstream of the current layer (J_z). The jet itself therefore does not act as a nozzle to limit the rate of reconnection: the rate of reconnection remains constant even as the length of the outflow jet varies in time.

To understand how the electrons can form such an extended outflow jet, we examine the out-of-plane compo-
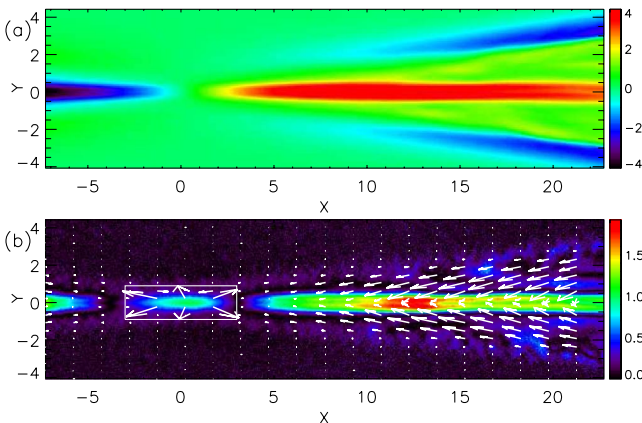
FIG. 3 (color online).   Blowups around the x line (averaged from $t = 172.5$ to 174.5) for the run in Fig. 2(a). In (a) The electron outflow velocity v_{ex}. In (b) Momentum flux vectors, $\mathbf{\Gamma} = p_{exz}\hat{\mathbf{x}} + p_{eyz}\hat{\mathbf{y}}$ (vectors in box surrounding x line are multiplied by 20), with a background color plot of $|[E_z + (\mathbf{v}_e \times \mathbf{B}/c)_z]/E_z|$.

nent of the fluid electron momentum equation along the symmetry line of the outflow direction. In steady state

$$E_z = -\frac{m_e v_{ex}}{e}\frac{\partial v_{ez}}{\partial x} - \frac{1}{c}v_{ex}B_y - \frac{1}{ne}\nabla \cdot \mathbf{\Gamma}, \quad (1)$$

where $\mathbf{v}_e$ is the electron bulk velocity, $\mathbf{\Gamma} = p_{exz}\hat{\mathbf{x}} + p_{eyz}\hat{\mathbf{y}}$ is the flux of z directed electron momentum in the reconnection plane (not including convection of momentum) with $\mathbf{p_e}$ the electron pressure tensor. In Fig. 4(a) we plot all of the terms in this equation along a cut though the x line along the outflow direction from a simulation with $m_i/m_e = 100$ and $L_x \times L_y = 102.4 \times 51.2$. The electric field (black) is balanced by the sum (red) of the electron inertia (dashed blue), the Lorentz force (solid blue) and the divergence of the momentum flux (green). The major contributions to momentum balance come from the Lorentz force and the divergence of the momentum flux. At the x line the electric field drive is balanced by the momentum transport [8,16]. The surprise is that the Lorentz force, rather than simply increasing downstream from the x line to balance the reconnection electric field, instead strongly overshoots the reconnection electric field far downstream of x line. This tendency was seen in earlier simulations [16] but there was no clear separation of scales because of the small simulation domain size. Downsteam from the x line the electrons are streaming much faster than the magnetic field lines. Thus, in a reference frame of the moving electrons the z directed electric field has reversed direction compared with the x line. This electric field tries to drive a
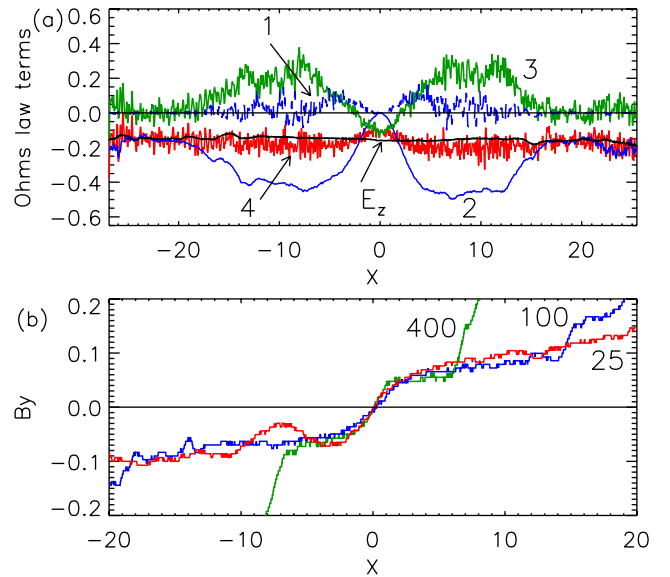
FIG. 4 (color online).   Results for simulation size 102.4×51.2 with $m_i/m_e = 25$ and 100; and 51.2×25.6 with $m_i/m_e = 400$. (a) Cuts through the x line (time averaged from $t = 116.2$ to 117.0) of the contributions to Ohm's law for $m_i/m_e = 100$. $1 \rightarrow -m_e/e\mathbf{v}_e \cdot \nabla v_{ez}$, $2 \rightarrow -\hat{\mathbf{z}} \cdot \mathbf{v}_e \times \mathbf{B}/e$, $3 \rightarrow -\hat{\mathbf{z}} \cdot (\nabla \cdot \mathbf{P_e})/(n_e e)$, $4 \rightarrow$ sum of 1, 2, 3. (b) Cuts through x line of B_y for the three different m_i/m_e.

current opposite to that at the x line. Evidence for this reversed current appears downstream of the x line in Fig. 2(c). In spite of the strength of the effective electric field, the reversed current carried by the electrons is small. As at the x line, the momentum transfer to electrons in this extended outflow region is balanced by momentum transport. The momentum flux around the x line is shown as a 2D vector plot in Fig. 3 for the same run as in (a). The background color plot is of $|[E_z + (\mathbf{v}_e \times \mathbf{B}/c)_z]/E_z|$, which is $\gtrsim 1$ where the electrons are not frozen-in. Evident is the outward flow of momentum around the x line and the much stronger outward flow of negative momentum in an extended downstream region. The momentum transport is sufficient to effectively block the out-of-plane current downstream. The force associated with this "blocking effect" drives the flow of the large-scale jet of electrons downstream of the x line.

We define the length Δ_x of the inner dissipation region as the distance from the x line to the point where the Lorentz force $v_{\mathrm{ex}}B_y/c$ crosses the reconnection electric field E_z. At this location the effective out-of-plane electric field seen by the electrons reverses sign, causing the electron current j_{ez} to be driven in reverse. This allows the separatrices to open up. Thus, the inner dissipation region defines the spatial extent of the magnetic nozzle that develops during reconnection. Since the simulations presented in this Letter use artificial values of m_e, it is essential to understand the m_e scaling of Δ_x so that this length can be calculated for a proton-electron plasma. The momentum equation of electrons in the outflow direction yields a steady state equation for v_{ex},

$$\frac{d}{dx}\left(\frac{1}{2}m_e v_{\mathrm{ex}}^2\right) = \frac{e}{c}v_{\mathrm{ez}}B_y, \qquad (2)$$

where $v_{\mathrm{ez}} \sim c_{\mathrm{Ae}}$. Thus, the profile of B_y along the outflow direction and its dependence on m_e must be determined. This profile is shown for three values of m_e in Fig. 4(b). Surprisingly, the profile of B_y is independent of m_e. Our original expectation was because of the continuity of the flow of magnetic flux into and out of the x line that $B_y \sim B_0 v_{\mathrm{in}}/c_{\mathrm{Ae}} \propto m_e^{1/2}$, where the outflow velocity eventually rises to c_{Ae}. However, since the electrons are not frozen into the magnetic field until far downstream, the expected scaling fails. To calculate v_{ex} we approximate B_y by a linear ramp and integrate Eq. (2). Setting the Lorentz force equation to the reconnection electric field, we then obtain an equation for Δ_x,

$$\Delta_x = \left(\frac{m_e}{m_i}\right)^{3/8}\left(\frac{cE_z}{B_0 c_A}\right)^{1/2}\left(\frac{B_0}{d_i B_y'}\right)d_i. \qquad (3)$$

For the three simulations shown in Fig. 4(b) Δ_x is given by $2.9d_i$, $1.8d_i$, and $1.0d_i$ for $m_i/m_e = 25$, 100, and 400, respectively, which is in reasonable accord with the scaling. Extrapolating to a mass-ratio of 1836, we predict $\Delta_x \sim$

$0.6d_i$. In contrast the outer dissipation region can extend to 10 s of d_i.

We have shown that the electron current layer that forms during reconnection stabilizes at a finite length, independent of the periodicity of the simulation domain, and aside from transients from initial conditions remains largely stable to secondary island formation. Reconnection remains fast with normalized (using the upstream variables) reconnection rates of around 0.12. The length of the electron current layer Δ_x scales as $m_e^{3/8}$. These simulations suggest that the formation of secondary islands is not a prerequisite for fast reconnection.

These rates of reconnection and the structure of the current layer are consistent with the results of recent (submitted around the same time as the present manuscript) large-scale, open-boundary simulations, where "quasi-steady" periods of reconnection arise even in the absence of secondary islands [17].

The structure of the current layer is important to the design of NASA's magnetospheric multiscale mission, which will be the first mission with the time resolution to measure the electron current layers that develop during reconnection. The length of the out-of-plane electron current layer projects to around c/ω_{pi} for a proton-electron plasma while the outflow jet, which supports a strong Hall (out-of-plane) magnetic field, extends 10s of c/ω_{pi} from the x line.

---

*shay@udel.edu
http://www.physics.udel.edu/~shay

[1] P. A. Sweet, in *Electromagnetic Phenomena in Cosmical Physics*, edited by B. Lehnert (Cambridge University Press, New York, 1958), p. 123.
[2] E. N. Parker, J. Geophys. Res. **62**, 509 (1957).
[3] M. A. Shay *et al.*, Geophys. Res. Lett. **26**, 2163 (1999).
[4] J. Birn *et al.*, J. Geophys. Res. **106**, 3715 (2001).
[5] A. Bhattacharjee *et al.*, Phys. Plasmas **12**, 042305 (2005).
[6] W. Daughton *et al.*, Phys. Plasmas **13**, 072101 (2006).
[7] K. Fujimoto, Phys. Plasmas **13**, 072904 (2006).
[8] M. Hesse *et al.*, Phys. Plasmas **6**, 1781 (1999).
[9] A. Zeiler *et al.*, J. Geophys. Res. **107**, 1230 (2002).
[10] D. Biskamp, *Magnetic Reconnection in Plasmas* (Cambridge University Press, Cambridge, England, 2000).
[11] M. A. Shay *et al.*, J. Geophys. Res. **106**, 3759 (2001).
[12] M. Hesse *et al.*, J. Geophys. Res. **106**, 29 831 (2001).
[13] J. F. Drake *et al.*, Geophys. Res. Lett. **33**, L13 105 (2006).
[14] M. A. Shay and J. F. Drake, Geophys. Res. Lett. **25**, 3759 (1998).
[15] M. Hoshino *et al.*, J. Geophys. Res. **106**, 25 979 (2001).
[16] P. L. Pritchett, J. Geophys. Res. **106**, 3783 (2001).
[17] H. Karimabadi *et al.*, Geophys. Res. Lett. **34**, L13 104 (2007).